Computational-Efficient Thermal Estimation for IGBT Modules under Periodic Power Loss Profiles in Modular Multilevel Converters

Zhang, Y.; Wang, H.; Wang, Z.; Blaabjerg, F.

Published in:
IEEE Transactions on Industry Applications

DOI (link to publication from Publisher):
10.1109/TIA.2019.2925590

Publication date:
2019

Document Version
Accepted author manuscript, peer reviewed version

This article has been accepted for publication in a future issue of this journal, but has not been fully edited. Content may change prior to final publication. Citation information: DOI 10.1109/TIA.2019.2925590, IEEE Transactions on Industry Applications

Computational-Efficient Thermal Estimation for IGBT Modules under Periodic Power Loss Profiles in Modular Multilevel Converters

Yi Zhang, *Student member, IEEE,* Huai Wang, *Senior member, IEEE,* Zhongxu Wang, *Student member, IEEE,* and Frede Blaabjerg, *Fellow, IEEE*

***Abstract*—One of the next challenges for modular multilevel converters (MMCs) is how to the size the critical components to its limits with reduced design margins, while at the same time fulfilling the reliability target. To do it confidently, better thermal modeling with quantitative uncertainty analysis is necessary to support the decision-making during the product design stage. Regarding conversion of long-term mission profiles into thermal profiles for reliability evaluation, this paper proposes a computational-efficient thermal modeling method for IGBT modules in MMCs. The proposed method considers the impact of the inherent thermal unbalance and has minimum computation with quantitative error analysis. Finally, both simulations and experiments have verified the theoretical results.**

***Index Terms*—Error analysis, insulated gate bipolar transistors (IGBTs), modular multilevel converters (MMCs), reliability, thermal analysis.**

I. Introduction

With modular multilevel converter (MMCs) having wide range of applications [1]–[4], its challenges of reliability are increasingly emerging. Although many redundancy schemes [5] and fault protection methods [6] are proposed to improve the reliability of the MMC, these methods usually sacrifices some important characters, such as cost, footprint, power density, etc. How to design an MMC to fulfill a specific reliability-target with compromised costs and design margins has not attracted so much attention yet. To do it confidently, better modeling methods with quantitative uncertainty analysis are necessary to support decision making at the design stage.

According to [7] and [8], junction temperature fluctuations are one of the dominant failure mechanisms for power semiconductor devices, which are classified into two types: 1) thermal cycles caused by the change of environmental conditions [9], [10], e.g., ambient temperature, wind speeds, solar irradiation, etc., and 2) periodic thermal profiles due to fundamental-frequency currents. As the amplitudes of periodic thermal profiles are relative moderate, some works usually ignored its effects in reliability evaluations [11]. However, [12]–[14] pointed out that a large number of minor thermal cycles have a non-negligible effect on the components fatigue. Moreover, high-power converters, e.g., MMC, have significant periodic thermal behaviors at the fundamental frequency. For instance, a 30-MW MMC has over 10°C temperature variations [15]. Therefore, the thermal behaviors under periodic power loss profiles should be considered carefully and estimated with a quantitative error.

In terms of the reliability evaluation of the MMC based on long-term mission profiles, one of the significant challenges is to convert tremendous periodic power loss profiles into thermal profiles. Many advanced simulation tools provide comprehensive thermal behavior analysis, such as the finite element method (FEM) and electro-thermal simulation (e.g., PLECS). However, these methods require massive computation; thus it is problematic to process a large number of power cycles (e.g., one-year mission profiles) for the reliability assessment. Following, some prior-art simplified thermal estimation models developed from two-level converters are computational light, such as the square-wave loss profile [16], the fixed half-sine loss profile [17], and the two-level power loss profile [13]. Nonetheless, these methods fail to consider the inherent thermal unbalance existing in the sub-module (SM) of the MMC. As a result, a large error might be introduced. Then, an equivalent power loss profile was proposed to consider the inherent thermal unbalance of the MMC in [15] and [18], but this method is still complicated to process a large number of thermal cycles efficiently. For instance, if the fundamental frequency is 50 Hz, there are approximately 10^9 periodic power cycles for one-year mission profiles. A heavy computational burden is still inevitable. Therefore, a further simplification of the equivalent power loss profile within a quantitative error level is demanding.

In this paper, a computational-efficient thermal estimation method is proposed for the IGBT modules of the MMC under periodic power loss profiles. An equivalent power loss profile is introduced in Section II to model the inherent thermal unbalance of the MMC. Then, Section III establishes a quantitative error model to simplify the equivalent power loss profile according to a maximum allowable error. Then quantitative error analysis helps to achieve a more confident reliability evaluation. Finally, the effectiveness of the proposed method is verified by simulations and experiments.

II. Configuration of the MMC and Thermal Estimation of Periodic Power Loss Profiles

This section introduces the configuration of the MMC at first. Then, in order to consider the varied thermal unbalance of the MMC, the equivalent power loss profile is summarized according to [15]. The challenge to further simplify the proposed equivalent power loss profile within a quantitative error is also introduced.

This article has been accepted for publication in a future issue of this journal, but has not been fully edited. Content may change prior to final publication. Citation information: DOI 10.1109/TIA.2019.2925590, IEEE Transactions on Industry Applications

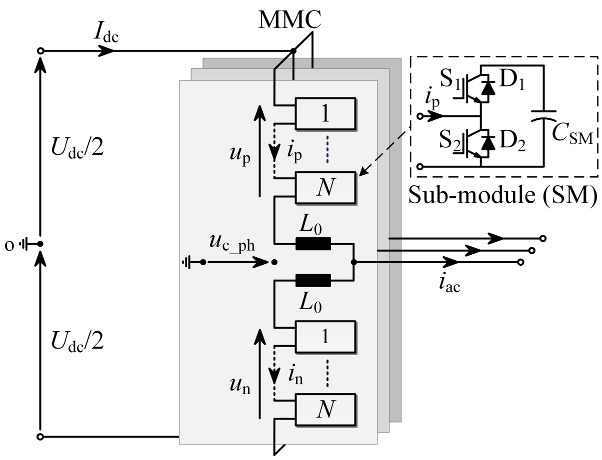

Fig. 1. Configuration of an MMC system (I_{dc} is the dc current, U_{dc} is the dc bus voltage, i_{ac} is the ac current, u_{p}, i_{p}, u_{n} and i_{n} are upper arm voltage/current and lower arm voltage/current, and $u_{\mathrm{c\_ph}}$ is the phase-voltage of the converter, respectively).

A. Configuration of the MMC and the Equivalent Power Loss Profile

As shown in Fig. 1, a typical three-phase MMC compromises six arms, and each arm consists of N SMs as well as an arm inductor L_0. In each SM, a half-bridge topology has two IGBTs (denoted as S_1 and S_2) and two free-wheeling diodes (D_1 and D_2).

In steady-state, the arm current of the MMC is mainly composed of a sinusoidal component at the fundamental frequency and a dc-bias current. An inherent power-loss unbalance is introduced by the dc-bias current, which leads to inherently unbalanced thermal behaviors in the power devices of the SM. Conventional methods [16], [17] developed from e.g. two-level converters cannot model the varied thermal unbalance of the MMC. Therefore, an equivalent power loss profile was proposed in [15], which is given by

$$P_{\text{equi\_inst}} = \begin{cases} P_{\text{peak}} \sin\left(2\pi f_e\right), & P_{\text{equi\_inst}} > 0 \\ 0, & P_{\text{equi\_inst}} \leq 0 \end{cases} \tag{1}$$

where P_{peak} is the amplitude of the equivalent power loss, and f_e is the equivalent frequency for characterizing the impacts of loss duration time. The process to obtain the parameters P_{peak} and f_e is illustrated in Fig. 2, which utilizes the zeros points and the average power losses to reconstruct an equivalent power loss profile. Accordingly, simplified thermal estimation can be achieved without the complicated instantaneous power loss profile.

Based on the zero points of the arm current, the equivalent frequencies are obtained by

$$\begin{cases} f_{\mathrm{e1}} = \dfrac{\pi}{\pi + 2\alpha} f_0, \ \text{for } \mathrm{D}_1,\, \mathrm{S}_2 \\ f_{\mathrm{e2}} = \dfrac{\pi}{\pi - 2\alpha} f_0, \ \text{for } \mathrm{S}_1,\, \mathrm{D}_2 \\ \text{where } \alpha = \arcsin\left(\dfrac{m\cos\varphi}{2}\right) \end{cases} \tag{2}$$

where parameter α varies with m and φ, indicating the unbalanced thermal behavior of the SM is varied with different

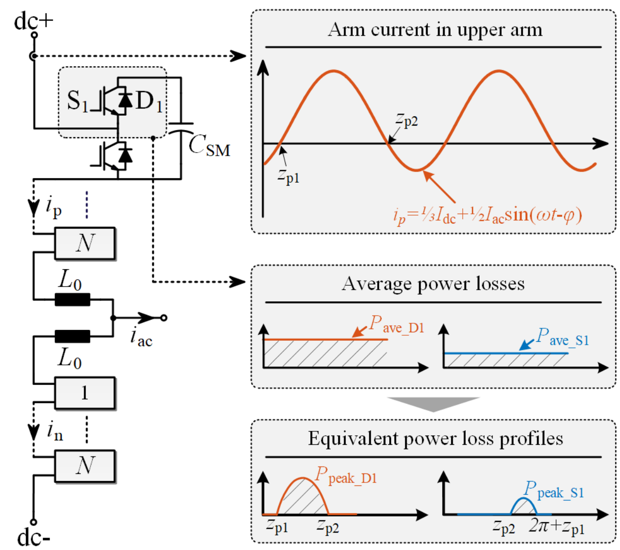

Fig. 2. Conversion from zero points of the arm current and the average power losses to reconstruct an equivalent power loss profile for the thermal estimation.

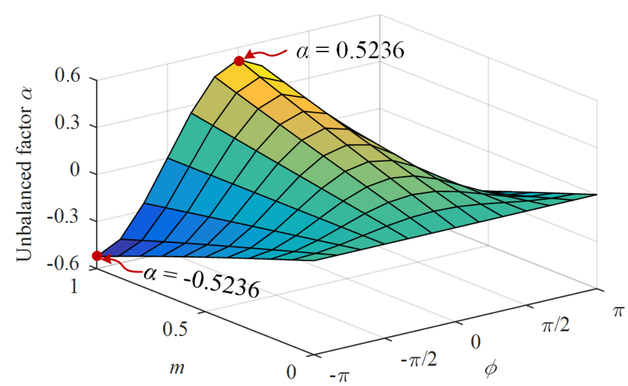

Fig. 3. The impact of the operational parameters (i.e., m and φ) on the thermal unbalance factor α: (a) 3D plot of the relationship, (b) α is varied with m and (c) α is varied with φ.

operational parameters of the MMC. As shown in Fig. 3, α reaches the peak when m = 1 and φ = 0, and the valley at m = 1 and $\varphi = \pm\pi$, namely the MMC has the largest thermal unbalance under these conditions.

Furthermore, P_{peak} is obtained by the same energy between the average power loss and the equivalent power loss. Taking the device S_1 as an example, which is

$$P_{\text{peak\_S1}} = \frac{\pi^2}{(\pi - 2\alpha)} P_{ave} \tag{3}$$

Therefore, the equivalent power loss profile for the MMC is established with the consideration of the inherent thermal unbalance.

B. Translation from Power Loss Profiles into Thermal Profiles

According to the thermal estimation model in [19], the obtained equivalent power loss profile should be divided into a series of square-wave dissipation pulses, where the junction

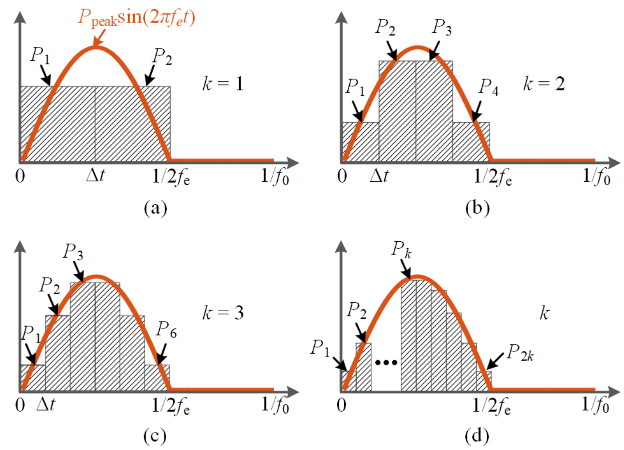

Fig. 4. Discretizing the equivalent power loss profile into a series of dissipation pulses, i.e., P_1, P_2, ..., P_k, ..., P_{2k} and k is the number of the divided dissipation levels: (a) one-level loss, (b) two-level losses, (c) three-level losses, (d) k-level losses.

temperature is estimated by an iterative equation given as

$$\begin{cases} \Delta T_{n-1} = P_{n-1} R_{\text{th}} \left(1 - e^{-\frac{\Delta t}{\tau_{\text{th}}}}\right) \\ \Delta T_n = \Delta T_{n-1} e^{-\frac{\Delta t}{\tau_{\text{th}}}} + P_n \sum\limits_{v=1}^{3} R_{\text{th}} \left(1 - e^{-\frac{\Delta t}{\tau_{\text{th}}}}\right) \end{cases} \tag{4}$$

where P_{n-1} is the previous dissipation, P_n is the actual dissipated power in each time step, R_{th} and τ_{th} are related to the thermal model and Δt is the time period of each separated dissipation pulse. A smaller Δt gives a more accurate power loss estimation, and thus a more accurate calculation of the temperature fluctuation but at the cost of more computations. However, the Δt is limited by the minimum time scale of the thermal model. In most data sheets, the time scale of the thermal impedances starts from 1 ms. Therefore, the most conservative way selects $\Delta t = 1$ ms to do the thermal estimation. In a one-year mission profile based lifetime prediction, a large number of power cycles under periodic power loss profiles are needed to be converted into thermal behaviors. If the fundamental frequency is 50 Hz and Δt = 1 ms is selected for the thermal estimation, around 10^9 cycles $\times$ 10 iterative equations are required to be computed. It is challenging to compute such a large amount of thermal cycles within a short period. Therefore, a further simplification of the thermal estimation with a quantitative error level is essential.

III. Simplification of Thermal Estimation with Quantitative Error Levels

This section proposes an analytical error model in terms of the estimation error and the number of divided dissipation pulses. The model targets to provide a minimum dissipation level for a given accuracy.

A. Discretization of the Proposed Equivalent Power Loss Profile and the Corresponding Error Model

As shown in Fig. 4, the equivalent power loss profile is divided into a series of dissipation pulses for thermal estimation. When k = 1, the equivalent power loss curve is simplified as a square wave consisting of P_1 and P_2 (see Fig. 4(a)). With the increase of k, the level of the discretized loss is increasing. Obviously, a larger k makes the discretized total power loss well approximated to the equivalent power loss profile, but at the cost of increasing computations. This indicates that an optimal point exist when the estimation is relatively accurate with the minimum computations.

Assuming that each dissipation pulse has the same energy as the equivalent power loss profile in the same time period, then each dissipation pulse can be expressed as

$$P_i = \frac{4k}{\pi} P_{\text{peak}} \sin\frac{\pi}{4k} \sin\frac{(2i-1)\pi}{4k} \tag{5}$$

where P_i is the i-th dissipation pulse amplitude, i = 1, 2, ..., $2k$, and P_{peak} refers to (3). Then, the pulse period is

$$\Delta t = \frac{1}{4 f_e k} \tag{6}$$

According to Fig. 4, the maximum dissipation pulses always lasts until the end of the $(k+1)$-th pulses, namely P_{k+1}. Thus, the maximum temperature can be achieved at the end of P_{k+1}. Substituting (5) into the thermal estimation equations (4), the maximum temperature is expressed as

$$\Delta T_{\max} = R_{\text{th}} \left(1 - e^{-\frac{\Delta t}{\tau_{\text{th}}}}\right) \begin{bmatrix} P_{k+1} \\ P_k \\ \vdots \\ P_1 \end{bmatrix}^{\text{T}} \begin{bmatrix} 1 \\ e^{-\Delta t/\tau_{\text{th}}} \\ \vdots \\ e^{-k\Delta t/\tau_{\text{th}}} \end{bmatrix} \tag{7}$$

which is simplified into

$$\Delta T_{\max} = \sum_{i=1}^{k+1} P_i R_{\text{th}} \left(1 - e^{-\Delta t/\tau_{\text{th}}}\right) e^{-(k+1-i)\Delta t/\tau_{\text{th}}} \tag{8}$$

According to (5) and (8), it is clear that a larger k or a smaller Δt gives a more accurate power loss estimation, and thus a more accurate thermal estimation. However, the lumped-RC thermal network, which is derived or calibrated based on experimental data, will be uncertain when predicting the transient response for the time shorter than these original measurements. It means the minimum Δt is limited by the minimum time scale of the experimental thermal network, which starts from 1 ms in most of the data sheets. Therefore, the maximum temperature fluctuation with Δt = 1 ms is considered as a valid base value, which is given as

$$\Delta T_{\max}(k_{\max}) = \sum_{i=1}^{k_{\max}+1} P_i R_{\text{th}} \left(1 - e^{\frac{-1}{4k_{\max} f_e \tau_{\text{th}}}}\right) e^{\frac{-(k_{\max}+1-i)}{4k_{\max} f_e \tau_{\text{th}}}} \tag{9}$$

where $k_{\max}$ is the maximum power loss level being $k_{\max} = \text{round}(1/(4f_e\Delta t)) = \text{round}(250/f_e)$.

Similarly, for arbitrary dissipation pulses with k levels, the maximum temperature fluctuation is expressed as

$$\Delta T_{\max}(k) = \sum_{i=1}^{k+1} P_i R_{\text{th}} \left(1 - e^{\frac{-1}{4k f_e \tau_{\text{th}}}}\right) e^{\frac{-(k+1-i)}{4k f_e \tau_{\text{th}}}} \tag{10}$$

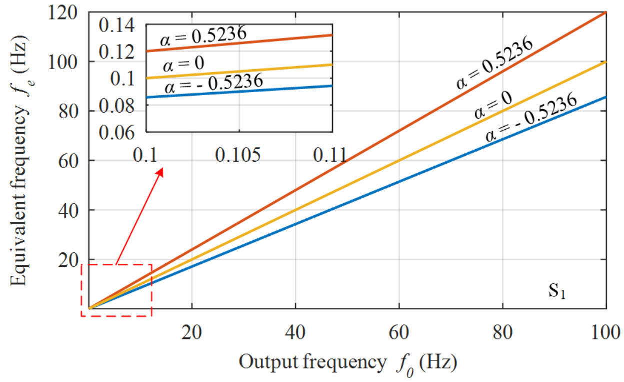

Fig. 5. The equivalent frequency range of the device S_1 when the output frequency ranges from 0.1 Hz to 100 Hz.

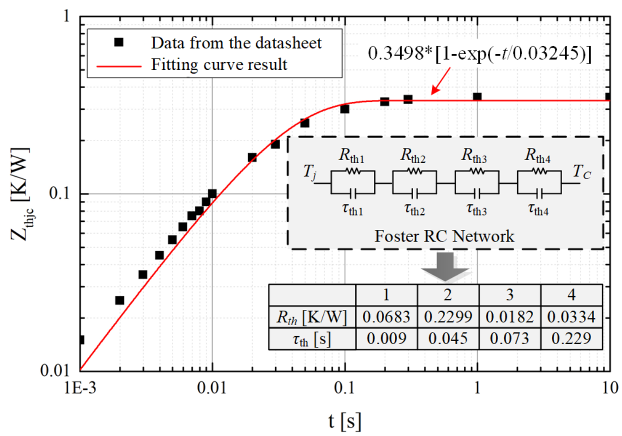

	1	2	3	4
R_{th} [K/W]	0.0683	0.2299	0.0182	0.0334
τ_{th} [s]	0.009	0.045	0.073	0.229

Fig. 6. Transient thermal impedances from the data-sheet and curve-fitted single-layer network, where T_j is the junction temperature, T_c is the case temperature, $R_{\text{th}i}$ is the thermal resistance and $\tau_{\text{th}i}$ is the thermal time constant.

Therefore, a relative error of the estimated temperature in respect to the base is defined as

$$\varepsilon = \frac{\Delta T_{\max}(k_{\max}) - \Delta T_{\max}(k)}{\Delta T_{\max}(k_{\max})}. \tag{11}$$

According to (9), (10) and (11), the obtained relative error is expressed as (12). The peak value of the equivalent power loss profile P_{peak} and the thermal resistance of the power device R_{th} are independent of the relative error. Hence, the relative error is only related to three parameters, one for the the number of loss level k, one for the frequency of the equivalent power loss profile f_e and one for the thermal time constant τ_{th}. Therefore, with a specific application (i.e., f_e and τ_{th} are known), the minimum dissipation level $k_{\min}$ can be calculated according to (12) with a pre-set maximum allowable error $\varepsilon_{\max}$.

B. A Case Study

In order to make the discretization of the equivalent loss profile clear, an IGBT module (1200 V/50 A, F4-50R12KS4) is chosen as the study case. In the following, the minimum required $k_{\min}$ is obtained based on three parameters: f_e, τ_{th} and $\varepsilon_{\max}$.

In typical applications, the fundamental frequency is 50/60 Hz. However, the frequency varies in some cases, such as machine drive [2], [20], sub-synchronous oscillation [21], etc. This paper considers the fundamental frequency ranging from 0.1 Hz to 100 Hz which covers most applications. According to (2), the equivalent frequency of device S_1 varies with the fundamental frequency and the unbalanced factor α as shown in Fig. 5. Thus, the equivalent frequency of S_1 has a range as

$$0.086 \leqslant f_e \leqslant 120, \text{ when } 0.1 \leqslant f_0 \leqslant 100. \tag{13}$$

Due to the thermal unbalance in the MMC, the equivalent frequency of the device S_1 is enlarged relatively to the fundamental frequency.

Furthermore, the thermal time constant refers to Fig. 6. A fourth-layer Foster network is provided in the datasheet of the selected IGBT module. However, the high-order thermal network is not straightforward to calculate the minimum dissipation level $k_{\min}$. As described in (12), a single-layer thermal time constant can be extracted from the high-order thermal network. Based on the curve fitting, the obtained thermal time constant is 0.03245 s for the selected IGBT module, which is also shown in Fig. 6. It should be noted that the curve-fitted single-layer thermal time constant is only utilized to obtain the minimum dissipation level. The thermal behavior estimation still relies on the thermal network provided in the datasheet, which can make sure that the multiple thermal time constants are covered simultaneously in the final thermal result.

Following, once a 10 % maximum allowable error is selected, Fig. 7(a) compares the resultant $k_{\min}$ and the correspondingly estimated thermal fluctuations under different equivalent frequencies. It is shown that $k_{\max}$ of the base increases exponentially when the equivalent frequency decreases. When the fundamental frequency is 0.1 Hz, the minimum equivalent frequency of the device S_1 had f_e = 0.086 Hz according to (11). Under the condition, the corresponding $k_{\max}$ is around 2,900, which is approximately 1,500 times larger than $k_{\min}$ = 2 under the same frequency. In contrast, $k_{\min}$ with the proposed method does not change significantly with the change of f_e. More specifically, when f_e varies from 0.086 Hz to 71 Hz, the temperature estimation can achieve a 10% error with $k_{\min}$ = 2 only. Once $f_e > 71$ Hz, $k = 1$ is enough to achieve the expected 10% error. The estimated temperature as shown in Fig. 7(a) indicates that the estimated temperature using $k_{\min}$ and $k_{\max}$ are very close. Additionally, Figs. 7(b) and (c) show the results when the $\varepsilon_{\max}$ is 5 % and 1 %, respectively. Compared with the results under 10 % maximum allowable error, the estimated temperature has better results under 5 % and 1 % errors at the cost of increasing of $k_{\min}$. However, $k_{\min}$ based on the proposed method is still very small compared to the $k_{\max}$ on the base value. As a larger k value means more iterative calculations in the thermal estimation, the proposed simplification method can reduce the computational burden significantly within a maximum allowable error.

C. Characterization of Thermal Behaviors of the MMC Under Periodic Power Loss Profiles

In order to clarify the proposed thermal method in long-term reliability evaluation, a flowchart of mission-profile-based

$$\varepsilon = 1 - \frac{\sum\limits_{i=1}^{k+1} k \sin\frac{(2i-1)\pi}{4k} \sin\frac{\pi}{4k} \left(1 - e^{\frac{-1}{4k f_e \tau_{\text{th}}}}\right) e^{\frac{-(k+1-i)}{4k f_e \tau_{\text{th}}}}}{\sum\limits_{i=1}^{k_{\max}+1} k_{\max} \sin\frac{(2i-1)\pi}{4k_{\max}} \sin\frac{\pi}{4k_{\max}} \left(1 - e^{\frac{-1}{4k_{\max} f_e \tau_{\text{th}}}}\right) e^{\frac{-(k_{\max}+1-i)}{4k_{\max} f_e \tau_{\text{th}}}}} \tag{12}$$

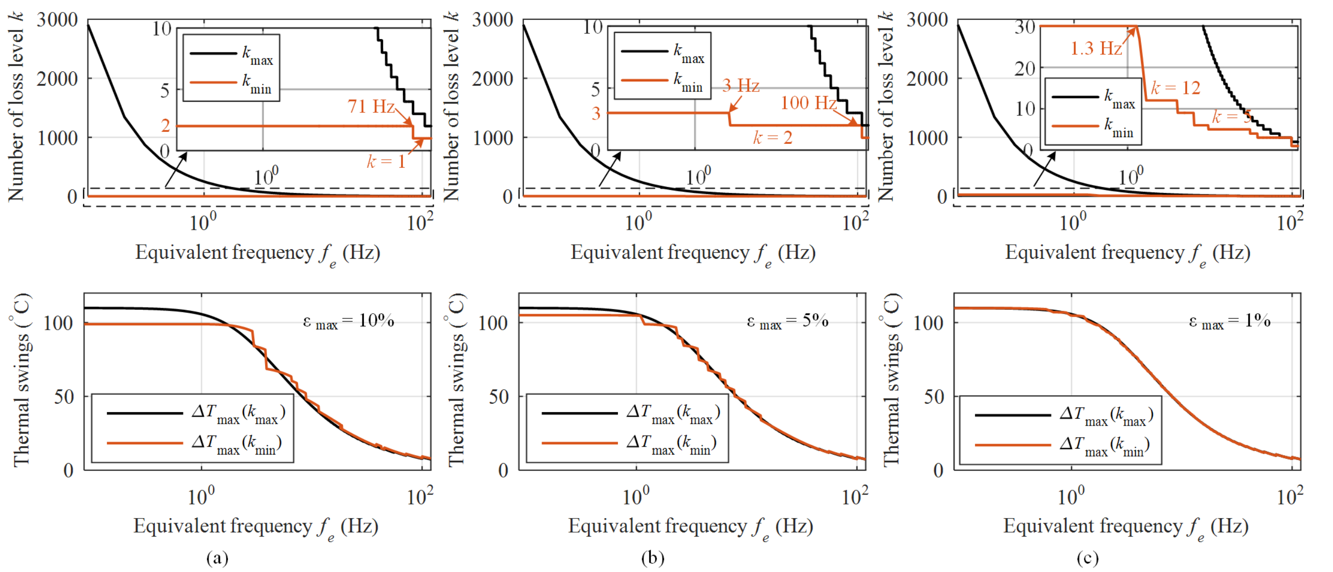

Fig. 7. Comparison between the base (Δt = 1 ms) and the proposed minimum number of loss levels within different maximum allowable errors under P_{ave}: (a) the loss level $k_{\max}$ according to base and the minimum loss level $k_{\min}$ according to the proposed method and their corresponding thermal fluctuations when $\varepsilon_{\max} = 10$ %, (b) when $\varepsilon_{\max} = 5$ % and (c) when $\varepsilon_{\max} = 1$ %.

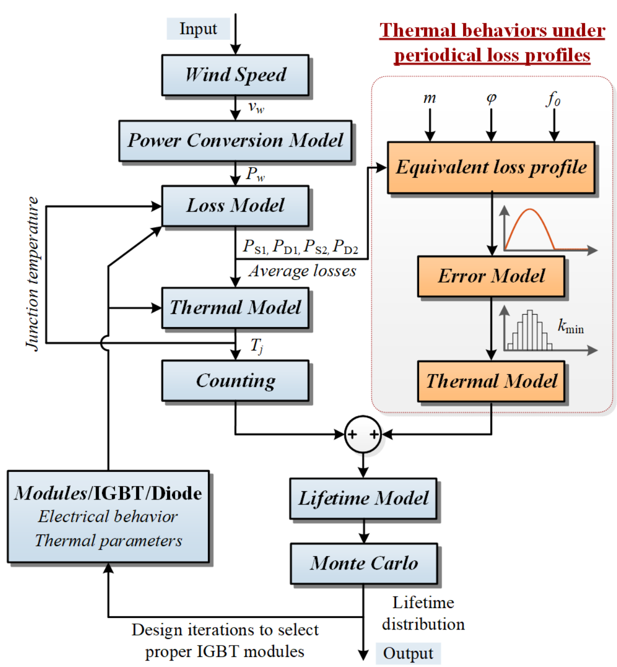

Fig. 8. Mission-profile-based lifetime prediction embedded with the proposed thermal estimation method under periodic power loss profiles, where the MMC is adopted to collect the wind power.

lifetime prediction method is shown in Fig. 8. The MMC system is assumed to collect the wind power. Thus, the mission profiles are annual wind-speed profiles, power profiles, loss profiles, etc. Once the average power losses are obtained (i.e., P_{S1}, P_{D1}, P_{S2} and P_{D2}), the equivalent power loss profiles are constructed according to (1), which can consider the inherent thermal unbalance of the MMC without the use of time-domain simulation. Afterward, the proposed quantitative error model of (12) provides the minimum required dissipation level $k_{\min}$ for thermal estimation. Therefore, the thermal behaviors of the power devices can be estimated with a minimum computation burden and a quantitative error level based on the proposed method.

IV. Validation by Experiments and Simulations

To verify the analysis above, the same IGBT module as in the case study is chosen. The validation characterizes the selected IGBT module at first to obtain the accurate loss information. Then, a platform is built up to test the thermal behaviors. Both experimental measurements and simulation validate the periodic thermal behaviors in terms of the low frequency, the high frequency, the steady state, and the transient state.

A. Characterization of the IGBT Module

The accuracy of thermal estimation depends on the accuracy of the power loss model. However, the information provided by IGBT datasheets is not comprehensively enough. For example, the provided power loss information lacks values under various temperatures and different blocking voltages. Moreover, the impact of the gate driver is not taken into account for the loss characterization. Therefore, the IGBT module should

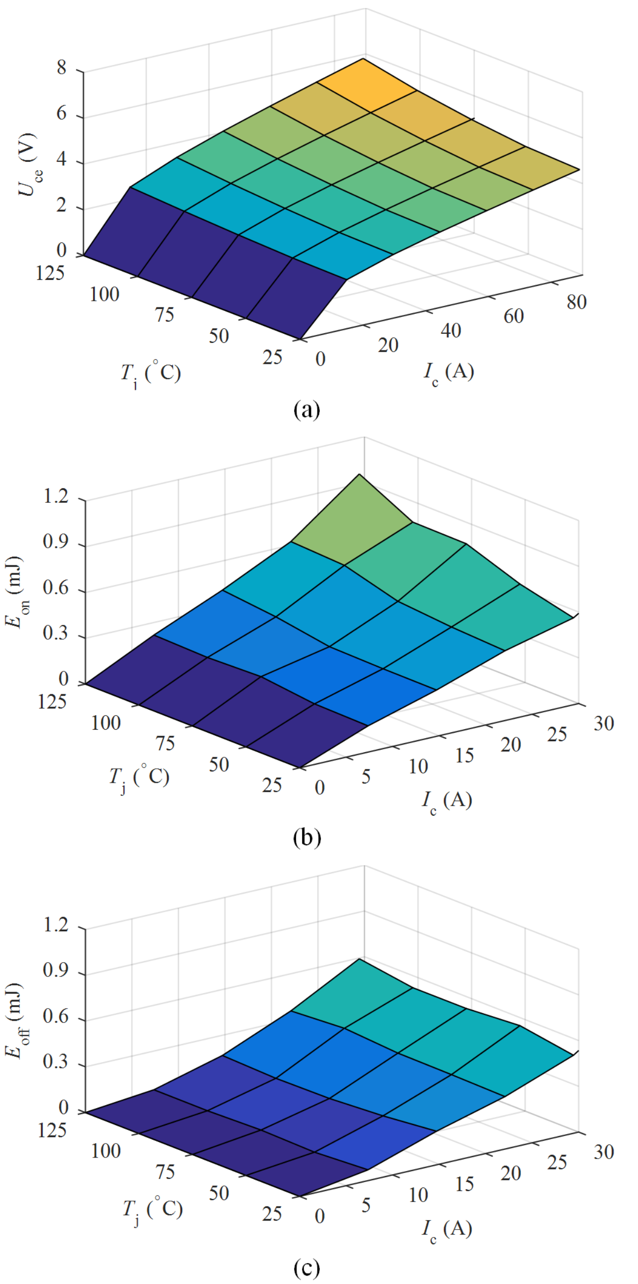

Fig. 9. Experimental characterization of the IGBT module at different temperatures: (a) output characteristic in on-state, (b) turn-on loss E_{on} and (c) turn-off loss E_{off}.

be characterized first to obtain the necessary power loss information.

The output characteristic of the IGBT reflecting the conduction loss is measured using Keysight B1506A curve tracer, where the temperature is controlled from 25°C to 125°C. Likewise, the switching losses are measured with a double-pulse circuit according to IEC60747-9, where a hot plate controls the device temperature. The measured results are shown in Figs. 9(a)-(c).

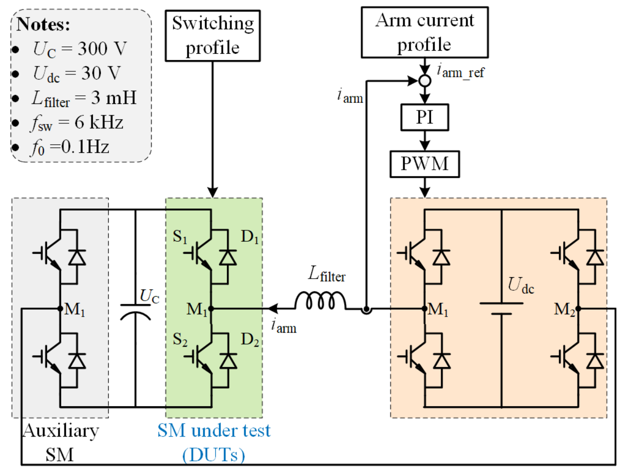

Fig. 10. Experimental platform for the thermal-behavior measurement in the MMC operation.

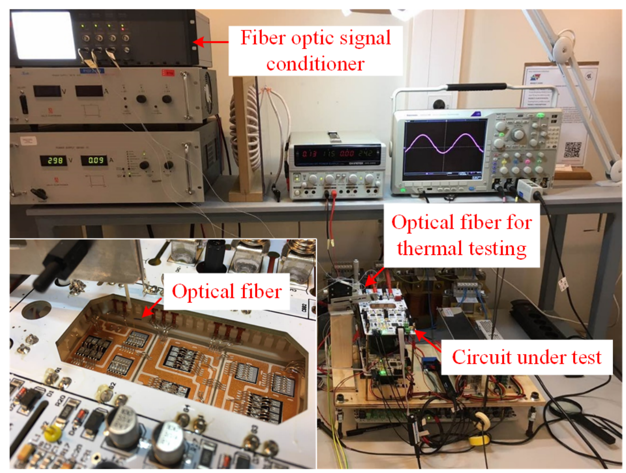

Fig. 11. The photo of the experimental platform.

B. Experimental Validation of the Steady-State Thermal Behaviors at 0.1 Hz

To measure the thermal behaviors of the power devices in the MMC, a platform is built as shown in Figs. 10 and 11, which is composed of three parts. The full-bridge circuit is employed to control the arm current like the MMC. The auxiliary SM is used to manage the capacitor voltage U_c as constant. Then, the switching profile is fed into the SM under test to emulate an SM working in an MMC system. The experimental platform has been introduced in [22] in detail. The thermal behaviors are measured by the Opsens thermal optical fibers [23].

Then, the measured junction temperature of S_1 is shown in Fig. 12. The junction-to-case temperature fluctuates like a half-sine wave, but the wave is not symmetrical in the period. This is because the loss duration time of S_1 is smaller than the half period of the fundamental-frequency cycle in the MMC. The obtained temperature fluctuation of S_1 is 6.84 °C in the experiment, and matches well with the time-domain simulated results as shown in Fig. 12(a). Based on the loss characterization above, the time-domain simulation can achieve an accurate temperature prediction, but the simulating method

This article has been accepted for publication in a future issue of this journal, but has not been fully edited. Content may change prior to final publication. Citation information: DOI 10.1109/TIA.2019.2925590, IEEE Transactions on Industry Applications

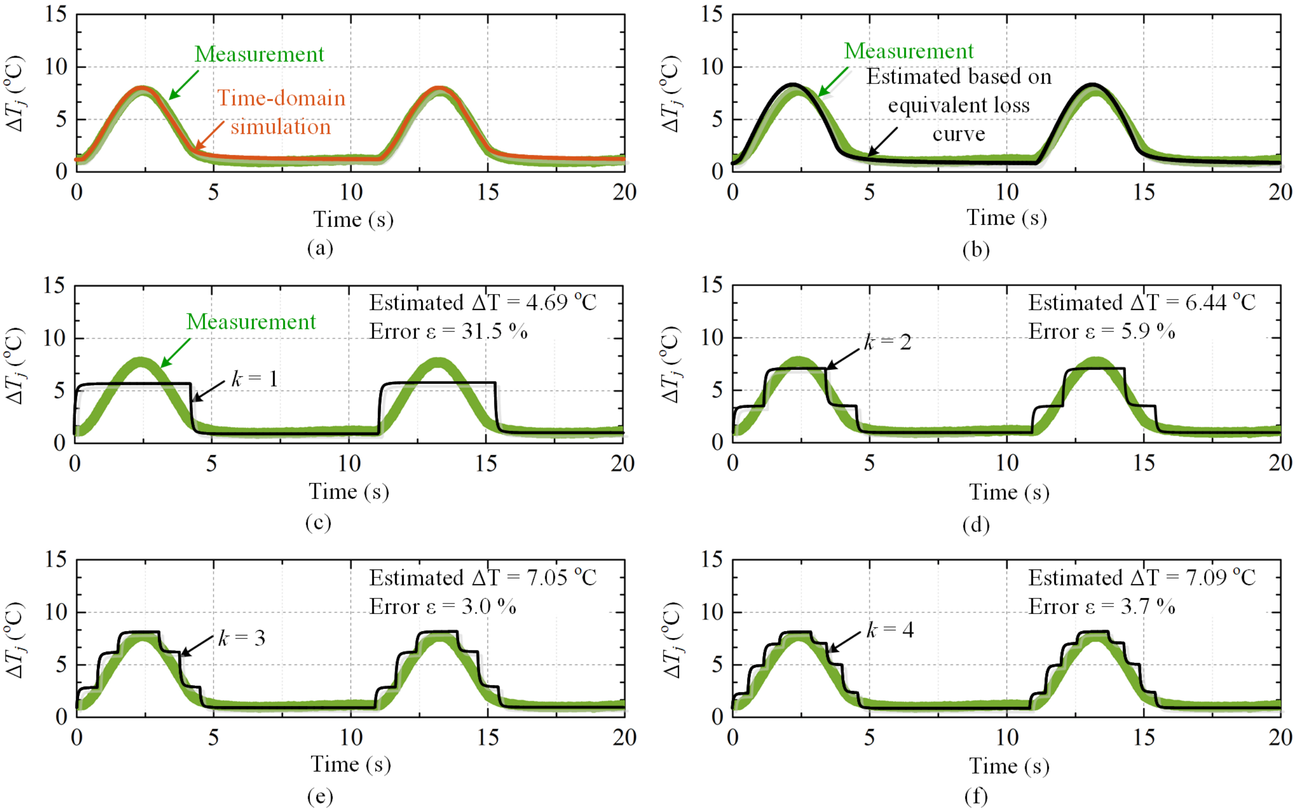

Fig. 12. Experimental comparison of the steady-state thermal behaviors based on the device S_1 at 0.1 Hz: (a) measurement and the time-domain simulation, (b) measurement and estimation based on the equivalent loss profile, (c) estimation based on the proposed method with loss dissipation k = 1, (d) based on $k = 2$, (e) $k = 3$ and (f) $k = 4$.

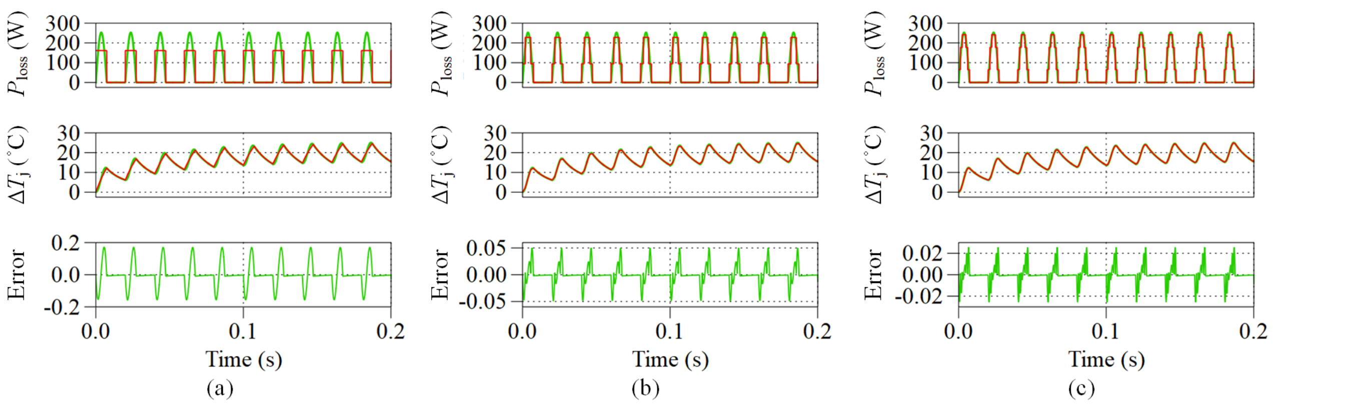

Fig. 13. Comparison of the power loss profiles, simulated thermal transient behaviors and the estimated error of the device S_1 at 50 Hz: (a) k = 1, (b) k = 2, and (c) k = 3.

is difficult to process long-term data for reliability evaluation. Following, as shown in Fig. 12(b), the equivalent power loss profile also provides a good thermal result compared to the measurement. It indicates that the equivalent loss profile can consider the thermal unbalance of the MMC well without the aid of time-domain simulation.

However, the equivalent power loss profile still requires a lot of computations to achieve thermal estimation by using (4). Thus, the proposed method provides further simplification as shown in Fig. 12(c)-(d). When $k = 1$, the estimated result is 4.69 °C, the relative error is around 31.5 %. By contrast, a 5.9 % error is achieved when $k = 2$. It corresponds to Fig. 7(a) where the dissipation level of $k = 2$ can achieve an $\varepsilon_{\max} = 10$ %. Likewise, both $k = 3$ and $k = 4$ reach into 5 % maximum of the allowable error but cannot go into 1 % error as shown in Fig. 12(e) and (f). The results verify that $k = 3$ is the minimum requirement to achieve a 5 % error but $\varepsilon_{\max} = 1$ % requires more dissipation levels, which has been analyzed in Fig. 7(b) and (c). Therefore, the proposed method is able to reduce the computational burden and meanwhile

This article has been accepted for publication in a future issue of this journal, but has not been fully edited. Content may change prior to final publication. Citation information: DOI 10.1109/TIA.2019.2925590, IEEE Transactions on Industry Applications

TABLE I
COMPARISON OF THERMAL ESTIMATION METHODS APPLIED TO THE MMC UNDER ONE-YEAR MISSION PROFILES WHEN THE FUNDAMENTAL FREQUENCY IS 0.1 HZ

	Number of iterations to process one-year mission profiles	Error relative to the measurement
The square wave profile [16]	3.15 $\times 10^6$	60.4 %
The half-sine profile [17]	1.58 $\times 10^{10}$	38.0 %
Two-level profile [13]	9.46 $\times 10^7$	44.0 %
Equivalent half-sine profile (Δt = 1 ms) [15]	1.16 $\times 10^{10}$	0.7 %
The proposed method (with 10 % error)	1.71 $\times 10^7$ (k = 2)	5.9 %
The proposed method (with 5 % error)	2.57 $\times 10^7$ (k = 3)	3.0 %

*Conditions: m = 0.8, φ = 0°, and the measured junction temperature variation is 6.84°C

to predict the thermal behaviors of the IGBT modules in the MMC within a quantitative error.

Furthermore, different thermal estimation methods applied to the MMC are compared in Table I. The conventional square-wave profile requires the minimum iterative computations to process one-year mission profiles, but the accuracy is the worst with an error of 60.4 %. Due to the ignorance of the thermal unbalance in the MMC, all three methods developed from two-level converters, such as the square-wave profile, the fixed half-sine profile and the two-level profile, are challenging to achieve good thermal estimation. Although the half-sine profile costs 1.58 $\times 10^{10}$ iterations, the estimated error is still 38.0 %. Following, the equivalent half-sine profile considers the thermal unbalance of the MMC; thus an error of 0.7 % is close to the results by time-domain simulation, but the computational burden is around 1.16 $\times 10^{10}$ iterations. For the proposed method in the paper, the dissipation level $k = 2$ is enough to achieve the error $\varepsilon_{\max} \leq 10$ % while the computation decreases to 0.1 % (i.e., 1.71 $\times 10^7$ iterations) of the equivalent half-sine profile. Moreover, the error of $\varepsilon_{\max} \leq 5$ % of thermal estimation if performed by k = 3, where the computation is 2.57 $\times 10^7$ only. Therefore, based on the proposed method, the computational burden for the thermal estimation can be reduced significantly while maintain within a quantitative error level.

C. Simulation Validation of the Transient Thermal Behaviors at 50 Hz

Due to the limited response time of the thermal sensors, the thermal behaviors at 50 Hz are validated by simulation. The simulation model and parameters are all the same as Fig. 10. The average power loss of the device S_1 intentionally increases to 50 W in the simulation to obtain a more obvious thermal response. As shown in Fig. 13, all the estimated thermal behaviors by k = 1, k = 2, and k = 3 can follow the transient thermal response by the equivalent half-sine profile. For the case with k = 1, the thermal error is more than 10 % as shown in Fig. 13(a). Then, the estimated error decreases to 5 % with k = 2 as shown in Fig. 13(b). Further increasing of the dissipation level to k = 3 as shown in Fig. 13(c), the estimated error decreases again to around 3 % but cannot achieve an error of 1 %. Therefore, both the transient responses and the estimated errors coincide well with the theory as shown in Fig. 7.

V. CONCLUSION

As IGBT modules in the MMC suffer from a large number of thermal fluctuations under periodic power loss profiles, it demands a method to estimate the thermal behaviors for lifetime prediction in terms of both accuracy and simplicity. This paper has proposed a computational-efficient thermal estimation method for periodic power loss profiles of MMCs, which consists of an equivalent power loss profile and a quantitative error model. The equivalent power loss profile serves to characterize the relationship between the unbalanced thermal behaviors of the MMC and the operational parameters (i.e., m, φ and f_0). Furthermore, a quantitative error model is adopted to simplify the equivalent power loss profile with a small number of computations. Based on the proposed method, the inherent thermal unbalances in the SM of the MMC can be modeled well without the aiding of time-domain simulation. The thermal estimation can be achieved by the minimum computations according to a given error level. Finally, an experimental platform has been built for validation. Both the experiments and simulations indicate that the proposed method effectively predicts the thermal behavior under periodic power loss profile of the MMC.

REFERENCES

[1] M. A. Perez, S. Bernet, J. Rodriguez, S. Kouro, and R. Lizana, “Circuit topologies, modelling, control schemes and applications of modular multilevel converters,” *IEEE Trans. Power Electron.*, vol. 30, no. 1, pp. 4–17, Mar. 2015.

[2] M. Hagiwara, K. Nishimura, and H. Akagi, “A medium-voltage motor drive with a modular multilevel PWM inverter,” *IEEE Trans. Power Electron.*, vol. 25, no. 7, pp. 1786–1799, Jul. 2010.

[3] H. Wang, G. Tang, Z. He, and J. Yang, “Efficient grounding for modular multilevel HVDC converters (MMC) on the AC side,” *IEEE Trans. Power Deliv.*, vol. 29, no. 3, pp. 1262–1272, Jun. 2014.

[4] M. Vasiladiotis and A. Rufer, “Analysis and control of modular multilevel converters with integrated battery energy storage,” *IEEE Trans. Power Electron.*, vol. 30, no. 1, pp. 163–175, Jan. 2015.

[5] G. Konstantinou, J. Pou, S. Ceballos, and V. G. Agelidis, “Active redundant submodule configuration in modular multilevel converters,” *IEEE Trans. Power Del.*, vol. 28, no. 4, pp. 2333–2341, Oct. 2013.

[6] O. Cwikowski, H. R. Wickramasinghe, G. Konstantinou, J. Pou, M. Barnes, and R. Shuttleworth, “Modular multilevel converter DC fault protection,” *IEEE Trans. Power Del.*, vol. 33, no. 1, pp. 291–300, Feb. 2017.

[7] S. Yang, A. Bryant, P. Mawby, D. Xiang, L. Ran, and P. Tavner, “An industry-based survey of reliability in power electronic converters,” *IEEE Trans. Ind. Appl.*, vol. 47, no. 3, pp. 1441–1451, Mar. 2011.

[8] ZVEL, “Handbook for robustness validation of automotive electrical/electronic modules,” Tech. Rep., Jun. 2008.

[9] Y. Zhang, H. Wang, Z. Wang, Y. Yang, and F. Blaabjerg, “The impact of mission profile models on the predicted lifetime of IGBT modules in the modular multilevel converter,” in *Proc. 43rd Annu. Conf. IEEE Ind. Electron. Soc.*, 2017, pp. 7980–7985.

[10] Y. Yang, E. Koutroulis, A. Sangwongwanich, and F. Blaabjerg, “Pursuing photovoltaic cost-effectiveness: Absolute active power control offers hope in single-phase pv systems,” *IEEE Ind. Appl. Magazine*, vol. 23, no. 5, pp. 40–49, Sep. 2017.

[11] H. Liu, K. Ma, Z. Qin, P. C. Loh, and F. Blaabjerg, “Lifetime estimation of MMC for offshore wind power HVDC application,” *IEEE J. Emerg. Sel. Topics Power Electron.*, vol. 4, no. 2, pp. 504–511, Sep. 2016.

[12] P. D. Reigosa, H. Wang, Y. Yang, and F. Blaabjerg, “Prediction of bond wire fatigue of IGBTs in a PV inverter under a long-term operation,” *IEEE Trans. Power Electron.*, vol. 31, no. 10, pp. 7171–7182, Dec. 2016.

[13] K. Ma, M. Liserre, F. Blaabjerg, and T. Kerekes, "Thermal loading and lifetime estimation for power device considering mission profiles in wind power converter," *IEEE Trans. Power Electron.*, vol. 30, no. 2, pp. 590–602, Mar. 2015.

[14] W. Lai, M. Chen, L. Ran, O. Alatise, S. Xu, and P. Mawby, "Low ΔT_j stress cycle effect in IGBT power module die-attach lifetime modeling," *IEEE Trans. Power Electron.*, vol. 31, no. 9, pp. 6575–6585, Nov. 2016.

[15] Y. Zhang, H. Wang, Z. Wang, Y. Yang, and F. Blaabjerg, "Simplified thermal modeling for IGBT modules with periodic power loss profiles in modular multilevel converters," *IEEE Trans. Ind. Electron.*, vol. 66, no. 3, pp. 2323–2332, Apr. 2018.

[16] A. Wintrich, N. Ulrich, T. Werner, and T. Reimann, *Application Manual Power Semiconductors*. Nuremberg, Germany: Semikron Int.GmbH, 2015.

[17] "Dimensioning program IPOSIM for loss and thermal calculation of Infineon IGBT modules," Infineon application notes, Tech. Rep.

[18] Y. Zhang, H. Wang, Z. Wang, and F. Blaabjerg, "Simplified estimation of the junction temperature fluctuation at the output frequency for IGBT modules in modular multilevel converters," in *Proc. IEEE Energy Convers. Congr. Expo. ECCE*, 2018.

[19] N. C. Sintamarean, F. Blaabjerg, H. Wang, F. Iannuzzo, and P. De Place Rimmen, "Reliability oriented design tool for the new generation of grid connected PV-inverters," *IEEE Trans. Power Electron.*, vol. 30, no. 5, pp. 2635–2644, May. 2015.

[20] A. Antonopoulos, L. Ängquist, S. Norrga, K. Ilves, L. Harnefors, and H. P. Nee, "Modular multilevel converter AC motor drives with constant torque from zero to nominal speed," *IEEE Trans. Ind. Appl.*, vol. 50, no. 3, pp. 1982–1993, May/Jun. 2014.

[21] Y. Liu, J. Sheng, Y. Dong, R. Zheng, and W. Li, "Thermal analysis of modular multilevel converters under subsynchronous oscillation," in *Proc. IEEE Energy Convers. Congr. Expo.*, Portland, 2018, pp. 5190–5195.

[22] Z. Wang, H. Wang, Y. Zhang, and F. Blaabjerg, "A viable mission profile emulator for power modules in modular multilevel converters," *IEEE Transactions on Power Electronics*, pp. 1–1, early access.

[23] OTG-F fiber optic temperature sensor. [Online]. Available: https://opsens-solutions.com/products/fiber-optic-temperature-sensors/otg-f/

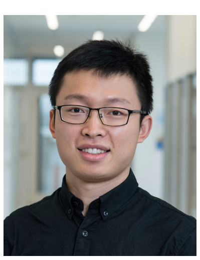

Yi Zhang (S'17) received the B.S. and M.S. degrees in electrical engineering from Harbin Institute of Technology, Harbin, China, in 2014 and 2016, respectively. He is currently working toward the Ph.D. degree with Aalborg University, Aalborg, Denmark. He was a visiting scholar with National Tsinghua University, Taiwan and Georgia Institute of Technology, USA in 2013 and 2018, respectively.

His current research interests include the reliability of power electronic devices and applications, and multilevel converters.

Huai Wang (M'12, SM17) received the B.E. degree in electrical engineering, from Huazhong University of Science and Technology, Wuhan, China, in 2007 and the Ph.D. degree in power electronics, from the City University of Hong Kong, Hong Kong, in 2012. He is currently an Associate Professor at the Center of Reliable Power Electronics (CORPE), and Vice Leader of Efficient and Reliable Power Electronics Research Program at Aalborg University, Aalborg, Denmark, and. He was a Visiting Scientist with the ETH Zurich, Switzerland, from Aug. to Sep. 2014, and with the Massachusetts Institute of Technology (MIT), USA, from Sep. to Nov. 2013. He was with the ABB Corporate Research Center, Switzerland, in 2009. His research addresses the fundamental challenges in modelling and validation of power electronic component failure mechanisms, and application issues in system-level predictability, condition monitoring, circuit architecture, and robustness design.

Dr. Wang received the Richard M. Bass Outstanding Young Power Electronics Engineer Award from the IEEE Power Electronics Society in 2016, and the Green Talents Award from the German Federal Ministry of Education and Research in 2014. He is currently the Chair of IEEE PELS/IAS/IE Chapter in Denmark. He serves as an Associate Editor of IET Electronics Letters, IEEE JOURNAL OF EMERGING AND SELECTED TOPICS IN POWER ELECTRONICS, and IEEE TRANSACTIONS ON POWER ELECTRONICS.

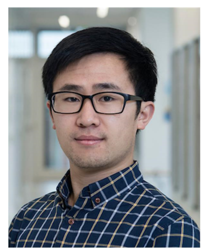

Zhongxu Wang (S'17) received his bachelor and master degrees in electrical engineering from Harbin Institute of Technology (HIT), China in 2014 and 2016 respectively. He is currently working towards his Ph.D. degree at Aalborg University, Denmark. In 2018, he was a visiting researcher with the Energy Futures Lab at Imperial College London, UK.

His research focuses on the reliability improvement strategies of modular multilevel converters, including power balancing control, adaptive control and condition monitoring of MMC.

Frede Blaabjerg (S'86, M'88, SM'97, F'03) was with ABB-Scandia, Randers, Denmark, from 1987 to 1988. From 1988 to 1992, he got the PhD degree in Electrical Engineering at Aalborg University in 1995. He became an Assistant Professor in 1992, an Associate Professor in 1996, and a Full Professor of power electronics and drives in 1998. From 2017 he became a Villum Investigator. He is honoris causa at University Politehnica Timisoara (UPT), Romania and Tallinn Technical University (TTU) in Estonia.

His current research interests include power electronics and its applications such as in wind turbines, PV systems, reliability, harmonics and adjustable speed drives. He has published more than 600 journal papers in the fields of power electronics and its applications. He is the co-author of four monographs and editor of ten books in power electronics and its applications.

He has received 30 IEEE Prize Paper Awards, the IEEE PELS Distinguished Service Award in 2009, the EPE-PEMC Council Award in 2010, the IEEE William E. Newell Power Electronics Award 2014 and the Villum Kann Rasmussen Research Award 2014. He was the Editor-in-Chief of the IEEE TRANSACTIONS ON POWER ELECTRONICS from 2006 to 2012. He has been Distinguished Lecturer for the IEEE Power Electronics Society from 2005 to 2007 and for the IEEE Industry Applications Society from 2010 to 2011 as well as 2017 to 2018. In 2019-2020 he serves a President of IEEE Power Electronics Society. He is Vice-President of the Danish Academy of Technical Sciences too.

He is nominated in 2014-2018 by Thomson Reuters to be between the most 250 cited researchers in Engineering in the world.